Biochemistry

Article

New Stereoselective Biocatalysts for Carboligation and Retro-Aldol Cleavage Reaction Derived from D-Fructose 6-Phosphate Aldolase

Huan Ma, Sarah Engel, Thilak Reddy Enugala, Derar Al-Smadi, Candice Gautier, and Mikael Widersten

Biochemistry, **Just Accepted Manuscript** • DOI: 10.1021/acs.biochem.8b00814 • Publication Date (Web): 11 Sep 2018

ACS Publications

is published by the American Chemical Society. 1155 Sixteenth Street N.W., Washington, DC 20036

New Stereoselective Biocatalysts for Carboligation and Retro-Aldol Cleavage Reaction Derived from D-Fructose 6-Phosphate Aldolase

*Huan Ma,† Sarah Engel, Thilak Reddy Enugala, Derar Al-Smadi, Candice Gautier‡ and Mikael Widersten**

Department of Chemistry – BMC, Uppsala University, Box 576, SE-751 23 Uppsala, Sweden.

KEYWORDS fructose 6-phosphate aldolase, biocatalysis, stereoselectivity, enzyme activity

ABSTRACT

D-fructose 6-phosphate aldolase (FSA) catalyzes the asymmetric cross-aldol addition of phenylacetaldehyde and hydroxyacetone. We conducted structure-guided saturation mutagenesis of non-catalytic active-site residues to produce new FSA variants, with the goal to widen the substrate scope of the wild type enzyme towards a range of *para*- and *meta*-substituted arylated aldehydes. After a single generation of mutagenesis and selection, enzymes with diverse substrate selectivity scopes were identified. The kinetic parameters and stereoselectivities for a subset of enzyme/substrate combinations were determined for the reactions in both the aldol addition and cleavage reaction directions. The achieved collection of new aldolase enzymes provides new tools for controlled asymmetric synthesis of substituted aldols.

INTRODUCTION

The aldol reaction is one of the most powerful methods for generating carbon-carbon bonds, building up the skeleton of organic molecules.[1] Hence, catalysts that facilitate these reactions in a stereo-controlled manner are highly desirable tools in synthetic chemistry. Current available catalysts for aldol reactions can be categorized into three groups: biocatalysts, small organic catalysts, *e.g.* proline, or metal coordinating complexes with chiral ligands.[2,3]

Table 1. Ketone and aldehyde substrates used for FSA catalyzed aldol addition

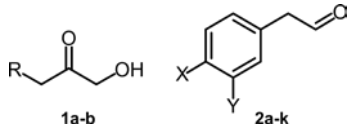

	substituent		
compound	R	X	Y
1a	H		
1b	OH		
2a		H	H
2b		CH_3	H
2c		OCH_3	H
2d		F	H
2e		Cl	H
2f		NO_2	H
2g		H	OCH_3
2h		H	F
2i		H	Cl
2j		H	NO_2
2k		OCH_3	OCH_3

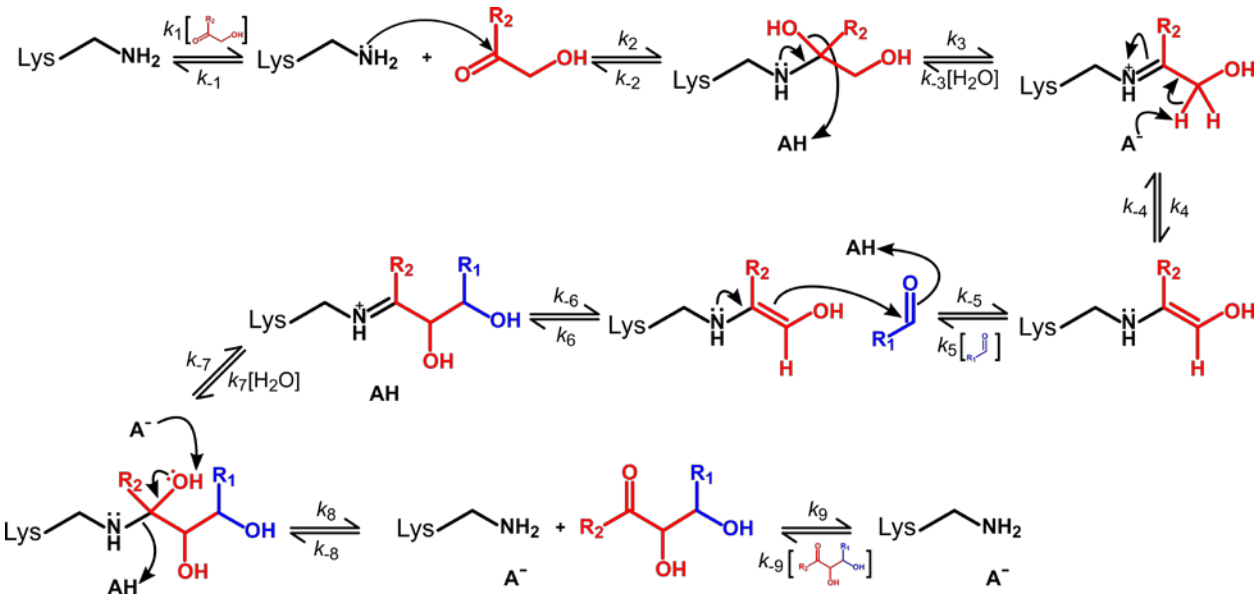

Figure 1. Outline of the mechanism of aldol addition catalyzed by Class I aldolases. An active site Lys (K85 in FSA) forms a Schiff base with the donor ketone substrate (red) following expulsion of water. Formation of the imine facilitates proton abstraction from the α-carbon and formation of the nucleophilic enamine that can react with the acceptor aldehyde (blue) to form the carbon-carbon bond, generating a new asymmetric center. The imine is subsequently hydrolyzed to release the aldol product.

In biological systems, aldolases are the enzyme catalysts for aldol reactions. These enzymes represent a special type of lyases that catalyze the reversible stereoselective addition of a donor nucleophile to an acceptor electrophilic compound[4] In most cases, the stereochemistry of the reaction product depends on the aldolase, therefore, these enzymes offer unique and environmentally friendly tools for biocatalysis of asymmetric carboligation.[1,5,6]

D-Fructose 6-phosphate aldolase (FSA) belongs to the Class I aldolase family and employs a catalytic lysine to generate a Schiff base intermediate after reaction with an incoming ketone.[7] The Schiff base facilitates deprotonation of the initial imine alcohol to generate a nucleophilic hydroxyenamine which reacts with acceptor aldehyde substrates (**Figure 1**). FSA is the first reported enzyme to reversibly cleave fructose 6-phosphate (F6P) generating glyceraldehyde 3-

phosphate (G3P) and dihydroxyacetone (DHA, **1b** in **Table 1**) *in vitro*[7,8] and the only enzyme, besides 2-deoxyribose-5-phosphate aldolase (DERA), to catalyze aldol reactions between two

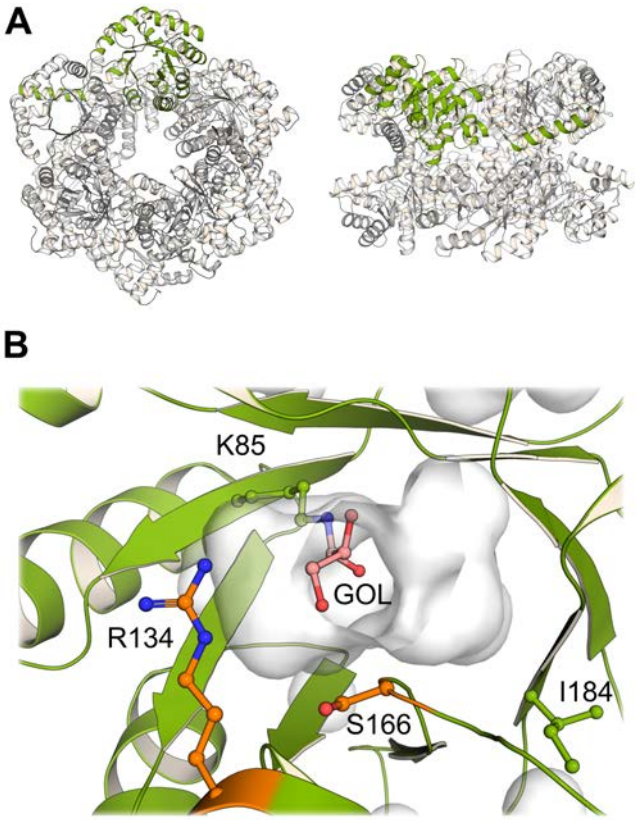

Figure 2. (A) The homodecameric structure of FSA is formed by intersubunit swapping of the C-terminal helix within a pentameric ring and stacking of the two rings. (B) Active-site cavity of FSA shown as a white surface. In the crystal structure, glyceraldehyde is covalently bonded to the catalytic K85 as a carbinolamine (carbons colored pink, GOL). The side-chains of residues R134 and S166 (carbons in orange), restrict the cavity volume and were therefore targeted for randomized mutagenesis. I184 is mutated to threonine in the R134I/S166G/I184T variant. Image created with PyMOL ver. 2.1[23] using the atomic coordinates in 1l6w.[11]

decamers consisting of two pentameric rings. The quaternary structure is stabilized by noncovalent forces also involving swapping of the C-terminal helix (**Figure 2A**).[11] The structure

renders FSA to be unusually thermostable for a mesophilic protein.[7] Unlike other Class I aldolases, FSA does not depend on phosphorylated donor substrates, a property that further increases its high potential as biocatalyst for aldol reactions in the production of polyhydroxylated compounds.[4,12] FSA has, to some extent, been integrated into organic synthesis and has also been engineered for different purposes, *i.e.* broader substrate scope for more general applicability.[13-21] Still, one persisting drawback with this enzyme is its relatively narrow range of accepted substrates. Wild type FSA has been reported to catalyze aldol addition of phenylacetaldehyde (**2a**) and hydroxyacetone (**1a**) (**Scheme 1**).[22]

Scheme 1. FSA catalyzed aldol reaction between phenylacetaldehyde (**2a**), and hydroxyacetone (**1a**). The formed product is (3*R*,4*S*)-3,4-dihydroxy-5-phenylpentan-2-one (**3a**).[22] The stereochemistry of the product is controlled by the enzyme.

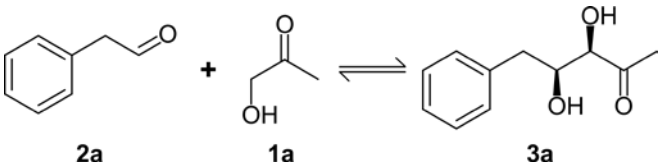

This basal enzymatic activity provides a good starting point for enzyme engineering aiming for improvements of catalysis of the same reaction but also for widening the scope of accepted derivative compounds.

Supported by the innate catalytic activity in the carboligation of **1a** and **2a**, we pursued structure-guided semi-rational mutagenesis of active site residues (CASTing[24]) to construct a library of enzyme variants. The side-chains of residues targeted for randomized mutagenesis, R134 and S166, are in the aldehyde acceptor binding region and interact via polar and hydrogen bond interactions with the phosphate group of either F6P or G3P.[11] The mutated residues are not involved in the catalytic mechanism (**Figure 2B**). The protein library was mined for new FSA

enzymes displaying higher retro-aldol activity with a racemic mixture of the *syn* diastereomers of aldol **3a**.

Hits were tested for their aldol addition activities with a spectrum of *para*- and *meta*-substituted phenylacetaldehydes (**Table 1**) in combination with either hydroxyacetone (**1a**) or dihydroxyacetone (**1b**). We can report the successful isolation of new enzymes that exhibit improved catalytic activity and high stereoselectivity in aldol addition reactions with overlapping but distinct substrate scopes. These enzymes provide new tools for asymmetric synthesis of polyhydroxylated compounds with defined stereo-configurations.

EXPERIMENTAL PROCEDURES

Chemicals and reagents – Synthetic oligonucleotides were purchased from Thermo Fisher Scientific GmbH (Ulm, Germany). B-PER (bacterial protein extraction reagent), all restriction enzymes, Taq DNA polymerase and supplement chemicals and buffers for molecular cloning were purchased from Thermo Fisher Scientific if not otherwise stated. The bacterial culture media components tryptone and sodium chloride were purchased from VWR, and Merck supplied agar and yeast extract. Nickel (II) Sepharose 6 Fast Flow gel for IMAC purification and disposable PD-10 desalting column were purchased form GE Healthcare Life Science. L-arabinose for protein expression induction, 96-well plate for both protein expression and library screening were purchased from VWR. EDTA-free protease inhibitor tablets were from Roche. All the other chemicals, antibiotics, buffer components were purchased from Sigma-Aldrich if not otherwise stated. Standard procedures and reaction conditions were used for gene cloning, and host cell transformations were performed as stated in the user manual from the manufacturers. DNA sequencing service was provided by Eurofins Genomics. Aldols **3a**, **3c**, **3e**

and **3m** (**Table 2**) were synthesized by reacting aldehydes **2a**, **2b**, **2c** and **2g**, respectively with methylglyoxal as described by Miyoshi *et al*..[25] The *syn* and *anti* diastereomer mixtures were separated by column chromatography and the *syn*/*anti* ratios were determined by NMR. Diastereomeric ratios are shown in **Table S3** in the **Supporting Information**. Substituted

Table 2. Structures of aldol products

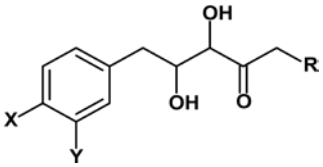

aldol	R	X	Y	aldol	R	X	Y
3a	H	H	H	**3m**	H	H	OCH_3
3b	OH	H	H	**3n**	OH	H	OCH_3
3c	H	CH_3	H	**3o**	H	H	F
3d	OH	CH_3	H	**3p**	OH	H	F
3e	H	OCH_3	H	**3q**	H	H	Cl
3f	OH	OCH_3	H	**3r**	OH	H	Cl
3g	H	F	H	**3s**	H	H	NO_2
3h	OH	F	H	**3t**	OH	H	NO_2
3i	H	Cl	H	**3u**	H	OCH_3	OCH_3
3j	OH	Cl	H	**3v**	OH	OCH_3	OCH_3
3k	H	NO_2	H				
3l	OH	NO_2	H				

phenylacetaldehydes **2b-2k** were synthesized by Wittig-type homologation from the corresponding benzaldehydes.[26] **2a** was purchased from Sigma-Aldrich and purified by chromatography. All aldehydes were ≥95 % pure before used, as judged by ^{1}H-NMR.

Library construction and screening – Over-lapping PCRs with mutagenesis primers were used to generate a library containing saturation mutations at codons R134 and S166, with the wild-type FSA (isoenzyme A) gene as template following the strategy by Tang *et al.*.[27] Primer sequences are given in **Table S2** in the **Supporting Information**. The generated PCRs fragments were inserted into the *Xho*I and *Spe*I sites of the expression vector pGT7-5His.[28] The library quality was estimated from sequencing 36 randomly picked clones.

The FSA mutant library (pGT7FSAR134XS166X-5His) was transformed into *E. coli* strain BL21-AI (Invitrogen) and plated on agar plates with 100 µg/ml ampicillin and grown overnight at 37 °C. 1260 single colonies were randomly picked and inoculated into 96-well round bottom plates. The controls included clones expressing wild type FSA, another (inactive) aldolase, DERA, and 2TY growth media. The cells were grown in 350 µl 2TY containing 100µg/ml ampicillin. The plates were then sealed with gas-permeable adhesive film and incubated at 37 °C overnight with shaking at 170 rpm. 50 µl of the overnight cultures were used to inoculate 300 µl fresh 2TY (with 50 µg/ml ampicillin) for protein expression. 55 µl of autoclaved 87 % (v/v) glycerol was added into the remaining 325 µl of overnight cultures, and these plates were stored at −80 °C for backup. The fresh inoculated expression cultures were incubated at 30 °C for ~7 h before 8 µl of 2 % L-arabinose solution was added (0.044 % (w/v) final concentration) to induce protein expression. The expression cultures were incubated at 30 °C overnight. Cells were harvested by centrifugation at 2191×*g* for 20 min at 4 °C. The supernatants were discarded. The 96-well plates containing the cell pellets were covered and stored at −80 °C until screening.

Frozen cell pellet in each well was resuspended in 25 µl B-PER with complete EDTA-free protease inhibitor tablets added. The plates were incubated for 1 h at room temperature with shaking at 170 rpm. 175 µl 50 mM triethanolamine (TEA) buffer, pH 8.0, was then added to each

well. The plates were centrifuged at 2191×*g* for 1 h at 4 °C. 75 µl clear lysate from each well was collected for screening of retro-aldol activity. The screening was performed essentially as described earlier[29] with the following differences: the screening reactions were performed in 0.1 mM NADH, 2 mM *rac*-**3a**, 0.44 µM FucO DA1472,[30] 35 µl cell lysate in 50 mM TEA buffer, pH 8.0 and 1 % (v/v) acetonitrile. Clones expressing an activity ≥1.5-fold as compared to wild-type control were scored as putative hits. Plasmids from hit clones were sequenced and these preliminary hits were re-screened after protein expression at 2-ml scale. The protein expression levels were analyzed by SDS-PAGE.

Expression and Purification of E. coli wild-type FSA and variants – Wild type FSA and enzyme variants from clones scored as displaying the relatively highest retro-aldol activity with *rac*-**3a** were expressed at larger scale and purified for kinetic analysis. Overnight cultures were prepared by inoculating frozen backup cultures of *E. coli* BL21-AI containing the plasmid for either the wild type, R134I/S166G/I184T, R134M/S166A or R134V/S166G variants, into 10 ml fresh 2TY growth medium (100 µg/ml ampicillin) and incubating at 37 °C overnight. The overnight cultures were used to inoculate 0.5 l fresh 2TY (50 µg/ml ampicillin) and the cultures were grown at 30 °C until OD_{600} reached ~0.8 when L-arabinose was added to 0.044 % (w/v). Protein expression was continued overnight at 30 °C. Cells were harvested by centrifugation at 3024×*g* for 15 min at 4 °C. The cell pellet was resuspended in IMAC Binding Buffer (10 mM sodium-phosphate, pH 7.5, 500 mM NaCl, 20 mM imidazole). The resuspended cells were lysed by ultrasonication and the lysate was subsequently centrifuged at 15,000×*g* for 40 min. The cleared supernatant was loaded onto 2 ml of a pre-equilibrated Ni(II)-Sepharose 6 Fast Flow gel. The loaded column was washed twice with 15 ml ice cold Washing Buffer (same composition as Binding Buffer but containing 60 mM imidazole). After washing, bound protein was eluted by

addition of 2.5 ml Elution Buffer twice (same composition as Binding Buffer but containing 300 mM imidazole). The protein solution obtained was desalted by passing through a PD-10 column equilibrated with 50 mM Gly-Gly buffer, pH 8.0. The purity of the protein was confirmed by SDS-PAGE stained with Coomassie Brilliant Blue R-250. The protein concentration of each variant was determined by measuring absorbance at 280 nm. The extinction coefficient of wild-type FSA at 280 nm was estimated from the amino acid composition using the ProtParam tool (www.expasy.org) to be 13,075 M^{-1} cm^{-1}.[31]

Substrate scopes – Reactions were carried out in the absence of light, at 30 °C and 75 rpm. The reactants were used in the following concentrations: 5 mM of aldehyde (**2a**-**k**) dissolved in acetonitrile (final concentration of 2.5 % (v/v)), 20 mM ketone (**1a**, or **1b**) and 25 µM of FSA or the variants in 50 mM TEA buffer pH 8. The total volume was 250 µl. All reactions were set up in duplicates. A blank without enzyme was prepared for every reaction and treated equally. Samples of 50 µl were taken after 8, 12 and 23 hours and each reaction was stopped by adding methanol to a final concentration of 50 %. The samples were then centrifuged 10 min at 16000×*g* and stored at −20 °C. Analysis was performed using an Ascentis™ C18, 25 cm x 4.9 mm column. The solvent system used was 50 mM sodium phosphate pH 3 (solvent A) and methanol (solvent B). An additional blank was prepared containing 5 mM aldehyde (**2a**-**k**) in acetonitrile. The injection volume was 10 µl and samples were eluted using a gradient elution from 40 to 90 % B over 35 min, with a flow rate of 0.5 ml min^{-1} and eluted compounds were detected by their absorption at 220 nm.

Kinetic characterization – Retro-aldol cleavage: Reactions were carried out in 50 mM TEA buffer, pH 8.0, 30 °C, at increasing concentrations of *rac*-**3a**, *rac*-**3e** and *rac*-**3m**. and in the presence of 0.83 µM FSA variant. The formation of the cleavage products **2a**, **2c** or **2g** was

monitored by reduction of the aldehyde by NADH (0.2 mM) catalyzed by an excess amount (~1 μM) of FucO DA1472.[29,30] The NADH consumption was monitored at 340 nm in a 0.5 cm cuvette. Steady state parameters were determined by fitting the Michaelis-Menten equation to the raw data using MMFIT and RFFIT in the SIMFIT package.[32] The activity of FucO DA1472 with aldehydes **2c** and **2g** was tested in advance to ensure that the coupling enzyme was added in adequate amounts to not interfere with the analysis of the retro-aldol activities of the tested aldolase enzymes.

Aldol addition: Reactions were performed, in triplicates, in 50 mM TEA buffer pH 8.0, 30 °C and 25 rpm. Increasing concentrations (0.5-5 mM) of **2a**, **2b** and **2c** were set up with 50 mM of the chosen ketone (**1a** or **1b**) and with 1 μM of enzyme. Aliquots were removed after 5, 10, 15 and 20 min and the reactions were terminated by addition of methanol (fortified with 2 mM of the internal standard 3-phenyl-1-propanol) up to a final concentration of 50 % (v/v). Samples were centrifuged for 10 min at 16,000×*g* and stored at −20 °C. Analysis was performed by reversed phase HPLC as described above. The peak areas of the products were normalized by the average area of the internal standard. For determination of the product concentration, calibration was made with increasing concentrations of reference aldol products. Steady state parameters were determined by fitting the Michaelis-Menten equation to the raw data using MMFIT and RFFIT.

Stereoconfiguration of aldol products – Selected product mixtures were separated on a Chiralpak AS-H (Daicel) using an isocratic mixture of *n*-hexane:isopropanol of 75:25 % (v/v) at a flow rate of 0.6 ml/min. The diastereomeric configurations were assigned from comparing the NMR spectra with those of known compounds (see the **Supporting Information** for details on scales of aldol syntheses and product work-up prior to NMR analysis) and after comparison with

analogous aldol derivatives synthesized by alternative methods. The chromatographic behavior described by Yang *et al.*[16] was also considered in the peak assignment.

RESULTS AND DISCUSSION

Library Screening – The FSA gene was mutated in a codon-unbiased randomized approach at codons R134 and S166. Mutated genes were expressed in *E. coli* and enzyme catalyzed retro-aldol cleavage of a racemic mixture of the *syn* diastereomers of **3a** was used as selection assay. The screening approach was based on the assumption that the cleavage of **3a** and the aldol addition of **1a** and **2a** are reversible. Thus, high catalytic activity in the retro-aldol reaction could suggest also an increased aldol addition activity. The coupled reaction used for assaying the cleavage of *rac*-**3a** also allows for facile screening of the activities of variant enzymes in a microtiter plate format.[29] The threshold for scoring 'hits' was set relatively low, 1.5-fold the activity displayed by the wild-type, to lower the risk of false negative results in the initial screening rounds. Out of 2400 screened clones, 42 (~2 %) were considered as hits (**Table S1**) and were re-screened. From the re-screen, three variants, R134I/S166G/I184T, R134M/S166A and R134V/S166G were deemed as most active in the retro-aldol cleavage of *rac*-**3** and were produced at larger scale, purified and characterized in further detail. These three selected variants all contain residue substitutions that introduce a hydrophobic residue at position 134 (M, I or V) combined with a small residue at position 166 (A or G). This is in line with that binding of the benzyl substituted aldol **3a** would benefit from a more non-polar active-site environment as compared to the methylene phosphate moiety of the suggested physiological substrates F6P and G3P. Interestingly, the R134V and S166G mutations have earlier been shown to be beneficial also for aldol addition of *N*-carboxybenzyl aminoaldehydes and **1a**, **1b** or glycoladehyde.[17]

Enzymatic activities – To assess the effects by the active-site substitutions in the isolated FSA variants a recapitulation of previous studies of the chemical and kinetic mechanisms is warranted. The catalytic mechanism of FSA has been proposed to depend on Y131 acting as general acid/base via a catalytic water molecule also hydrogen bonded to Q59 and T109 (**Figure S1**).[8,16,33,34] Site-directed mutagenesis of Y131 into phenylalanine, however, does not affect the aldol reaction between **1a** and cinnamaldehyde derivatives negatively,[16] nor do hydrogen-bond breaking mutations at Q59, which questions the importance of these residues to catalysis. The activities of some Q59 mutants are even improved over that of the wild type, an effect mainly due to increases in V_{max}. In contrast, the same Y131F mutation is detrimental to the aldol addition of **1b** and G3P.[8] A proposed role of Y131 is as catalytic acid facilitating dehydration of the initial carbinolamine, forming the Schiff base.[33] It appears as if the former reactions where hydroxyacetone is the ketone donor is less dependent on the Y131 contribution as compared to the reaction involving dihydroxyacetone. Another cause of the observed differences may be drastically different rate limiting steps in the aldol additions between **1a** and cinnamaldehyde as compared to the reaction between **1b** and G3P rendering the former reaction less sensitive to loss of this catalytic residue. The Y131F mutation abolishes the activity in the retro-aldol cleavage of F6P.[16] Thus, it appears as if Y131 is required in the reactions involving the physiological(?) substrates F6P and G3P but is less critical in reactions involving **1a** as donor. The mechanism proposed by Stellmacher and coworkers invokes a role as general base abstracting the proton from the C-4 hydroxyl of F6P.[8] The importance of a Tyr residue at that position is further supported by the fact that an F178Y substitution, inserting the phenol functionality in a spatially similar position in the structurally related transaldolase TalB, introduces FSA-like aldolase activity.[35]

The kinetic mechanism of FSA has not been extensively studied but is expected to follow a strictly ordered model analogous to fructose 1,6-*bis*-phosphate aldolase,[36] although the identity of catalytic residues differ between these isoenzymes.[34] In this model, the ketone donor reacts first to form the Schiff base, via a carbinolamine intermediate. The ketimine is subsequently deprotonated to the nucleophilic enamine that reacts with an incoming aldehyde forming the aldol (**Figure 1**). The rate limiting step of FSA catalyzed retro-aldol or aldol addition reactions have not been determined which is problematic when interpreting kinetic data and evaluating effects by residue substitutions. An assumed 'slow' step would be abstraction of the α-proton from the Schiff base carbon acid to form the reactive enamine (with rate constant k_4 in **Figure 1**). However, if this is a rate limiting step the pH dependence of k_{cat} would to some extent reflect the pK_a of the protonated α-carbon. To our knowledge, the pH dependence of k_{cat} with any combination of ketone and aldehyde has not been reported. Stellmacher *et al.* describe the pH dependence of the specific activity, assayed at sub-saturating concentrations of **1b** ($1.6\times K_M$) and G3P ($3.5\times K_M$) that suggests a single ionization event with an apparent pK_a of approximately 7.[8] This is four pH units more acidic than the pK_a estimated for the corresponding acetone ketimine[37] and is better matched by the acidity of the deprotonation of the K85 ammonium group, which displays a pK_a of 5.5.[8] A modest deuterium kinetic isotope effect observed with the rabbit fructose 1,6-*bis*-phosphate aldolase also speaks against the enamine formation to be rate determining in that case.[36] If the pH dependence of k_{cat} follows that of K85 ionization, the rate of formation of the carbinolamine intermediate formed after attack of the Lys amine on the donor ketone (or aldol), with rate constant k_2 (or k_{-8}), may be rate limiting. That a step prior to deprotonation of the Schiff base should be rate limiting is also suggested for fructose 1,6-*bis*-phosphate aldolase. The central role of the bound water molecule is invoked from its

conspicuous location close to the reactant and a catalytic role for water has also been implied from solvent deuterium kinetic isotope effects on fructose 1,6-*bis*-phosphate aldolase.[36]

Interpretation of steady-state kinetic parameters – The Michaelis constant is the apparent equilibrium dissociation constant for the sum of all enzyme-substrate intermediate species occurring on the pathway up to the production of the (first) product.[38] In the retro-aldol reaction this would include all steps from binding and stabilization of the ground state enzyme-aldol complex and the stabilization of the carbinolamine and Schiff base. Hence, the value of K_M may be misleading regarding information about binding affinity in the initial Michaelis complex. Similarly, in the aldol addition $K_M^{aldehyde}$ will in addition to the enzyme-aldehyde dissociation constant ($K_s^{aldehyde}$; k_{-5}/k_5), depend on the degree of accumulation of the enzyme-ketimine Schiff base and the enamine. Consequently, changes in K_M may reflect alterations in the stabilities of intermediates and thereby rather provide some crude estimate of effects on microscopic rates of chemical steps instead of changes in enzyme-aldehyde interactions.

The turnover (k_{cat}) numbers reflect rate limiting steps and reasons for an observed increase in k_{cat} as a consequence of mutagenesis can be due to either that (a), introduced substitutions have lowered the energy barrier for the rate limiting reaction step, *e.g.* increased stabilization of the carbinolamine, which in an extreme case may shift the rate limitation step to a step that was previously not rate limiting, or (b), the relative proportion of productive over nonproductive substrate binding has been increased. One diagnostic of the latter cause is that K_M increases to the same extent resulting in unchanged values of k_{cat}/K_M.[38,39] These possible mechanisms were taken into account in the analysis of the here isolated FSA variants.

Retro-aldol cleavage reactions – The isolated enzymes were initially tested for their retro-aldol activities with the screening substrate *rac*-**3a**. The activity displayed by wild type FSA is similar

to what has been reported for the retro-aldol cleavage of F6P, albeit measured under slightly different conditions.[7,8]§ This is noteworthy considering the drastically different structures of these substrates and suggests a degree of substrate promiscuity. Of the isolated FSA variants, both R134M/S166A and R134V/S166G display increased turnover numbers (**Table 3**), with an 11-fold increase in the case of R134V/S166G. However, since also the K_M values increase to similar extents the overall catalytic efficiencies, expressed as k_{cat}/K_M, are essentially unchanged with this substrate if compared to the wild type. It should be noted that since the aldols tested as substrates are not enantiopure; in the cases of **3a** and **3m** the activities were determined with racemic mixtures of the *syn* diastereomers, it can not be excluded that one of the enantiomers acts as a competitive inhibitor. This should, however, not affect the values of k_{cat} but the determined values of k_{cat}/K_M should be considered to represent lower limits of activity. With **3e**, also the presence of the *anti* diastereomers may further influence the analysis since either stereoisomer may act as either susbtrate or inhibitor.

The underlying cause of the k_{cat} increase is at this stage speculative but the concomitant elevations of both k_{cat} and K_M suggest that the higher rate results from an increase in the ratio of productive *versus* nonproductive substrate binding. The k_{cat} values of the R134V/S166G and R134M/S166A variants also explain why these clones were originally scored as hits in the screening process given the substrate concentration in the assay (2 mM), although their k_{cat}/K_M values are not substantially higher than the wild type value. The purified R134I/S166G/I184T variant does not exhibit an increase in its catalytic activity with *rac*-**3a** which suggests that the apparent higher activity of this clone in the screening was due to elevated expression levels. The R134I/S166G/I184T enzyme was still included in the following characterization due to its structural relationship with the more active R134V/S166G variant.

Table 3. Steady state kinetic parameters for retro-aldol cleavage of *rac*-**3a**, *rac*-**3e** and *rac*-**3m**

enzyme	k_{cat} (s^{-1})	K_M (mM)	k_{cat}/K_M ($s^{-1}\times M^{-1}$)
wild type / **3a**[a]	1.6±0.1	3.6±0.5	440±40
R134V/S166G / **3a**[a]	18±4	28±7	640±30
R134I/S166G/I184T / **3a**[a]	1.7±0.06	5.0±0.3	340±9
R134M/S166A / **3a**[a]	3.5±0.1	7.5±0.5	470±10
wild type / **3e**[b]	0.93±0.1	12±2	77±5
R134V/S166G / **3e**[b]	9.1±2	15±4	610±60
R134I/S166G/I184T / **3e**[b]	8.0±3	32±10	250±20
R134M/S166A / **3e**[b]	7.4±1	13±3	570±40
wild type / **3m**[a]	0.59±0.03	9.5±0.8	62±2
R134V/S166G / **3m**[a]	7.9±2	9.0±3	870±100

[a] >99 % *syn* diastereomers. [b] 59:41 % *syn*:*anti* diastereomers.

When tested for retro-aldol cleavage of the *p*-methoxy derivative (*rac*-**3e**) the R134V/S166G variant again displayed approximately 10-fold improved turnover rate as compared to the wild type enzyme (**Table 3**) with a similar improvement also in k_{cat}/K_M. The same positive effect on activity is also observed with the *m*-methoxy aldol (*rac*-**3m**); the R134V/S166G mutant displays a 14-fold increase in k_{cat}/K_M mainly due to a higher turnover number (**Table 3**). Also the R134M/S166A and R134I/S166G/I184T variants show k_{cat} values similar to R134V/S166G with *rac*-**3e**. The $K_M^{\mathbf{3e}}$ displayed by the R134I/S166G/I184T variant is increased approximately two-fold as compared to the other enzymes.

Aldol addition reactions – The primary aim of the initial mutagenesis and screening process was to isolate FSA variants that had acquired improved aldol addition activities. To assess this, the wild type and the R134I/S166G/I184T, R134M/S166A and R134V/S166G FSA variants

were challenged to catalyze aldol addition of a spectrum of 11 phenylacetaldehydes (**2a**-**2k**) in combination with ketones **1a** or **1b** (**Table 1**). The resulting complete data set is shown in **Figure S2.** The different enzyme variants exhibit a range of activities with the different aldehyde and ketone combinations with some observations that stand out: (1) the R134V/S166G variant displays the highest degree of product formation with *p*-methoxyphenylacetaldehyde (**2c**). The difference to the wild type being largest when combined with dihydroxyacetone (**1b**) as donor ketone (**Figure 3A**). In general, the R134V/S166G variant displays the overall broadest substrate scope. (2) The R134M/S166A variant exhibit highest activity with the *p*-methylphenylacetaldehyde (**2b**) in combination with **1b**, and with the disubstituted **2k** combined with **1b** (**Figure 3B, C**). (3) The wild type enzyme display lower activities when the aldehyde is combined with **1b** as compared to hydroxyacetone, **1a**. This observation agrees with earlier studies of FSA variants in the addition of **1a** or **1b** to also other aldehydes.[13,17] The steady state data presented by Castillo *et al.* points towards that the difference lies mainly in the values of k_{cat}. Interestingly, an A129S substitution can increase the turnover number with **1b** to the same level as with hydroxyacetone.[13] Furthermore, *para*-fluorophenylacetaldehyde (**2d**) in combination of either ketone is a relatively poor substrate for all tested enzymes. **Figure S3D** shows representative elution profiles of the reaction mixtures catalyzed by the R134V/S166G variant after 23 hours incubation. The amount of unreacted aldehyde (later eluting peaks in the chromatogram) is substantial also after such extensive reaction time. A similar result is observed with the dimethoxy substituted **2k** when combined with **1b**. The elution profile shown in **Figure S3K** is that of the R134M/S166A catalyzed reaction mixture after 23 hours. Although this variant displays the highest apparent activity with this substrate combination, a relatively large amount of aldehyde remains in the mixture. Judging from the time-dependencies of formed

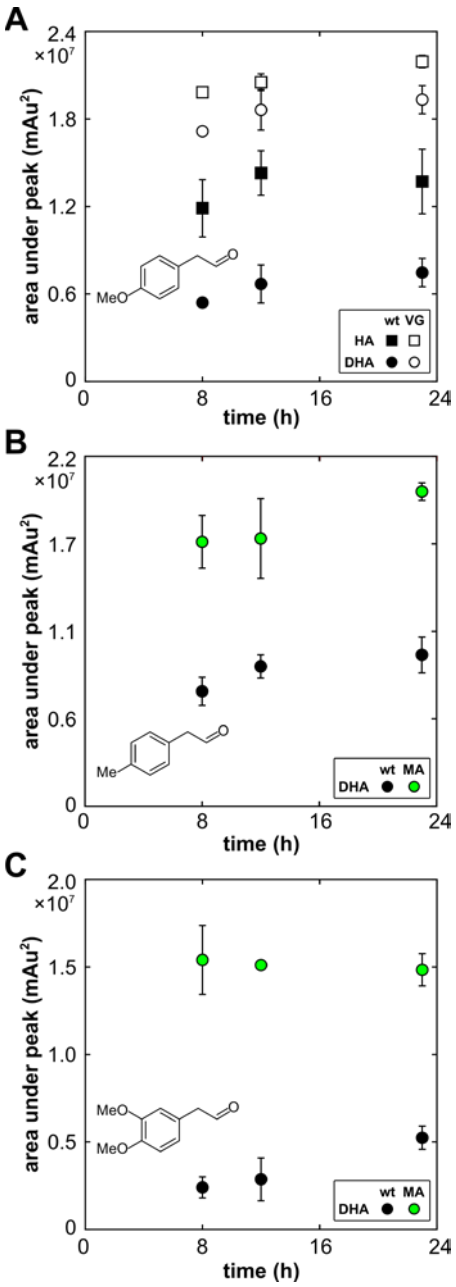

Figure 3. Formation of aldol addition product as a function of time. 5 mM aldehyde was reacted with 20 mM ketone in the presence of 25 µM of FSA variant at pH 8. (A) Difference in catalyzed aldol product formation between wild type (filled symbols) and the R134V/S166G variant (unfilled symbols) with aldehyde **2c** and either ketone **1a** (squares) or **1b** (circles). (B) Difference in catalyzed aldol product formation between wild type (black circles) and the R134M/S166A variant (green circles) with (B), aldehyde **2b** and ketone **1b** and (C), with aldehyde **2k** and ketone **1b**. Error bars show the standard deviation, n=2.

Table 4. Steady state kinetic parameters for aldol addition

enzyme	product	k_{cat}[a] (s^{-1})	K_m[a] (mM)	k_{cat}/K_m[a] ($s^{-1}\times M^{-1}$)
wild type / **1a + 2a**	**3a**	2.2±0.2	6.8±3	320±40
R134V/S166G / **1a + 2a**	**3a**	1.7±0.2	2.7±1	620±100
wild type / **1b + 2a**	**3b**	0.99±0.3	11±4	93±10
R134V/S166G / **1b + 2a**	**3b**	0.49±0.1	4.5±2	110±20
wild type / **1b** + **2b**	**3d**	0.11±0.06	9.1±7	12±3
R134M/S166A / **1b** + **2b**	**3d**	0.78±0.7	23±20	33±5
wild type / **1a + 2c**	**3e**	0.18±0.06	5.5±4	33±9
R134V/S166G / **1a + 2c**	**3e**	0.35±0.04	0.91±0.4	390±100
wild type / **1b + 2c**	**3f**	>0.01[b]	>2.5[b]	2.5±0.6
R134V/S166G / **1b + 2c**	**3f**	0.035±0.005	2.4±0.8	14±3

[a] 'Apparent' parameter values determined in the presence of 50 mM ketone (**1a** or **1b**) and varied concentrations of aldehyde, at pH 8, 30 °C. [b] Not adequate enzyme saturation within the used aldehyde concentration range.

aldol products, the amounts of remaining aldehyde and in the presence of the most efficient catalysts, the aldol reactions appear to have reached their equilibrium states with the exceptions of the mentioned reactions producing **3g**, **3h**, and **3v** (**Figures S3 and S3**). In aqueous solution these aldehydes exist as equilibrium mixtures of the hydrated *gem*-diol and the carbonyl forms. Thus, the observed reaction rates will depend on the relative amounts of these different species and the catalytic activity of the enzyme at hand with the respective aldehyde substrates. In the reaction between either the *meta*- or *para*-nitrophenylacetaldehydes (**2f** and **2j**) and **1a** a side product eluting slightly later with the main aldol product peaks is observed. The amount of this side product is approximately 30 % irrespective of the enzyme variant that has been used for catalysis. We have not been able to conclusively determine the structure of this side product but

speculate that it may be the 1,4-dihydroxy-5-(3 or 4-nitro)-pentane-2-one isomer based on its identical UV-vis spectral properties to the main aldol peak and the fact that this side product is not present in the corresponding reactions with the symmetric **1b** ketone (**Figure S3F, J**). Guided by these results, the steady state kinetic parameters were determined for a chosen set of variants and substrate combinations (**Table 4**). In general, k_{cat} decreases in all tested enzymes when substituents are added to phenylacetaldehyde. The wild type displays a ~10-fold decrease in turnover number with *p*-methoxy substituted (**2c**) together with **1a** and similarly with the *p*-methyl substituted (**2b**) in combination with ketone **1b**.

In general, the effects by the substitutions differ from those observed in the retro-aldol reactions. Increases in k_{cat}/K_M are mainly due to lower K_M values in the formation of **3a**, **3b**, **3e** and **3f**, although also increases in k_{cat} are observed; the higher catalytic efficiency of the R134M/S166A enzyme in the formation of **3d** is solely due to a 7-fold increase in turnover number. These distinct behaviors in the steady state kinetics suggest that different steps of the catalyzed reaction pathway have been affected by the substitutions *and* for different substrate pairs. Furthermore, changing the ketone donor from **1a** to **1b** results in all tested cases in that k_{cat}/K_M drops significantly. In the reaction with **1b** and **2c** this effect is caused primarily because k_{cat} decreases by one order of magnitude but less so in the comparison with **1a**/**1b** and **2a**. Possibly the *para*-substitution causes sterical constrains that impedes appropriate geometry between the enamine and the incoming aldehyde acceptor substrate. This notion, although speculative, is supported by the somewhat increased $K_M^{\mathbf{2c}}$ values in the reactions with **1b**.

It should also be noted that the reactions were measured in the presence of constant concentrations of donor ketones, the estimated values for k_{cat} and k_{cat}/K_M should therefore be viewed as apparent and represent lower limit values. However, when the assay was tested in the

presence of 50 or 100 mM of donor ketone, there was no increase in enzyme activity at the higher ketone concentration why 50 mM was considered to be adequately saturating.

Stereoconfiguration of aldol products – The enzymatically produced aldols all display exclusively the *syn* configuration of the asymmetric centers as suggested by the similarity of the NMR spectra (**Figure S5**) with the corresponding spectra of close analogs with known structures.[22] The coupling constants of the ^{1}H-NMR signals of the protons bound to the chiral carbons further support this assignment; the coupling constants, and the NMR spectra, of the enzymatically synthesized **3d** are identical to the *syn* diastereomers of the same compound synthesized using SmI_2[25] but distinct from those of the *anti* diastereomers (**Table S3**). Enzymatically produced aldols **3d**, **3e**, **3f** and **3n** all elute as single peaks under HPLC conditions which separate the two possible *syn* enantiomers demonstrating enantiopure products (**Table S3**, **Figure S6**). In the case of **3e** reference compounds synthesized using SmI_2 were available which aids in the elucidation of the stereoconfigurations. The biocatalytically produced **3e** coelutes with the first eluted peak in chiral chromatography, which agrees with the elution profile of the FSA catalyzed product between cinnamaldehyde and **1a** which has been determined to be (3*R*,4*S*).[16] Crystallization attempts of these enzyme produced compounds have been initiated to conclusively establish their absolute stereoconfigurations.

CONCLUSIONS

Aldolase catalyzed transformations of asymmetric polyhydroxylated compounds are powerful additions to the synthetic toolbox. The synthesis of the aldols presented in this work can be achieved also by other methods utilizing transition metals or organocatalysts.[25,40] The products generated by these methods, however, are mixtures of stereoisomers and require further

purification steps for optical purity. In comparison, the enzyme catalyzed aldols described here are of high enantiopurity, without need for further purification steps depending on yet unclear but relief of unproductive binding may be a cause of the higher k_{cat} with *rac*-**3a**, whereas in the case of *rac*-**3e** and *rac*-**3m**, the data rather suggest that the rate limiting step has been accelerated since the effect is mainly on k_{cat} and k_{cat}/K_M. In the aldol addition reactions, the rate acceleration in the reactions with **2c** and either ketone is mainly expressed in k_{cat}/K_M and due to lowering of $K_M^{\mathbf{2c}}$. This behavior can be caused by an increased stabilization of either the ternary complex or the preceding Schiff base or enamine. However, if formation of the Schiff base is rate limiting for the aldol reaction, an elevation of k_{cat} would be expected, which is not observed. This points towards that either stabilization of the enamine or the ternary Michaelis complex are the main causes for the higher values of k_{cat}/K_M.

To conclude, we have isolated aldolase variants with increased catalytic aldol addition activities with a range of *para* and *meta*-substituted phenylacetaldehydes. The enzymes were identified from a protein library of active-site mutants screened for retro-aldol activity with *rac*-**3a**. Although the used screening strategy is not directly linked to the desired aldol addition activities, and that the retro-aldol reactions may follow alternative kinetic mechanisms, the successful isolation of the described enzyme variants suggests that the applied screening approach is able to identify enzymes of improved activities. The improvements in the aldol addition reactions are, however, more modest as compared to the corresponding retro-aldol reactions. Test synthesis of four different aldols demonstrate the applicability of these enzymes for synthesis of enantiopure polyhydroxylated aldols adding to existing examples of the FSA substrate scope.[13-22, 33]

ASSOCIATED CONTENT

Supporting Information. Experimental details on NMR analysis, supplementary tables: hits from library screens, oligonucleotide sequences, supplementary figures: substrate scope in aldol addition reactions, chemical formulae, NMR spectra, chiral separations.

AUTHOR INFORMATION

Corresponding Author

* E-mail: mikael.widersten@kemi.uu.

Present Addresses

† Biovica International AB. Dag Hammarskjölds väg 54B, Uppsala Science Park, SE-752 37, Uppsala, Sweden.

‡ Department of Biochemical Sciences "Alessandro Rossi Fanelli", Sapienza University of Rome, 00185, Rome, Italy.

Author Contributions

The manuscript was written through contributions of all authors. All authors have given approval to the final version of the manuscript.

Notes

§ The enzyme activities reported by Schürman & Sprenger (2001) are expressed as units/mg of enzyme which translates to k_{cat} values for the retro-aldol cleavage of F6P of 2.7 s^{-1} and 17 s^{-1} for the aldol addition of **1b** and G3P. The corresponding values reported by Stellmacher *et al.*, (2015) are 2.3 s^{-1} and 8 s^{-1}, respectively.

ACKNOWLEDGMENT

The authors thank Lara Pfaff, Marianne Mühlbacher and Nastassia Knödlseder for contributing to data collection and professor Thomas Norberg for critical reading of the manuscript. The work was supported by Stiftelsen Byggmästare Olle Engkvist and The Carl Trygger Foundation. We are also grateful to COST action 1303 Systems Biocatalysis for support. SE was an Erasmus+ Scholarship recipient.

REFERENCES

(1) Machajewski, T. D., and Wong, C. H. (2000) The Catalytic Asymmetric Aldol Reaction. *Angew. Chem. Int. Ed. 39*, 1352-1374.

(2) Mahrwald, R. (2004) Modern Aldol Reactions Vol. 1, Wiley-VCH. Weiheim, ISBN 3527307141.

(3) Trost, B. M., and Brindle, C. S. (2010) The Direct Catalytic Asymmetric Aldol Reaction. *Chem. Soc. Rev. 39*, 1600-1632.

(4) Samland, A. K., and Sprenger, G. A. (2006) Microbial Aldolases as C–C Bonding Enzymes – Unknown Treasures and New Developments. *Appl. Microbiol. Biotechnol. 71*, 253-264.

(5) Fessner, W. D., and Helaine, V. (2001) Biocatalytic Synthesis of Hydroxylated Natural Products Using Aldolases and Related enzymes. *Curr. Opin. Biotechnol. 12*, 574–586.

(6) Clapés, P. and Garrabou, X. (2011) Current Trends in Asymmetric Synthesis with Aldolases. *Adv. Synth. Catal. 353*, 2263-2283.

(7) Schürman, M., and Sprenger, G. A. (2001) Fructose-6-phosphate Aldolase Is a Novel Class I Aldolase from *Escherichia coli* and Is Related to a Novel Group of Bacterial Transaldolases. *J. Biol. Chem. 276*, 11055-11061.

(8) Stellmacher, L., Sandalova, T., Leptihn, S., Schneider, G., Sprenger, G. A., and Samland, A. K. (2015) Acid–Base Catalyst Discriminates Between a Fructose 6-Phosphate Aldolase and a Transaldolase. *ChemCatChem 7*, 3140-3151.

(9) Garrabou, X., Castillo, J. A., Guérnard-Hélaine, C., Parella, T., Joglar, J., Lemaire, M., and Clapés, P. (2009) Asymmetric Self- and Cross-Aldol Reactions of Glycolaldehyde Catalyzed by D-Fructose-6-phosphate Aldolase. *Angew. Chem. Int. Ed. 48*, 5521-5525.

(10) Sánchez-Moreno, I., Nauton, L. Théry, V., Pinet, A., Petit, J.-L., de Berardinis, V., Samland, A. K., Guérard-Hélaine, C., and Lemaire, M. (2012) FSAB: A New Fructose-6-Phosphate Aldolase from *Escherichia coli*. Cloning, Over-Expression and Comparative Kinetic Characterization with FSAA. *J. Mol. Catal. B Enzym. 84*, 9-14.

(11) Thorell, S., Schürmann, M., Sprenger, G. A., and Schneider, G. (2002) Crystal Structure of Decameric Fructose-6-Phosphate Aldolase from *Escherichia coli* Reveals Inter-subunit Helix Swapping as a Structural Basis for Assembly Differences in the Transaldolase Family. *J. Mol. Biol. 319*, 161-171.

(12) Castillo, J. A., Calveras, J., Cassas, J., Mitjans, M., Vinardell, M. P., Parella, T., Inoue, T., Sprenger, G. A., Joglar J., and Clapés, P. (2006) Fructose-6-phosphate Aldolase in Organic Synthesis: Preparation of D-Fagomine, N-Alkylated Derivatives, and Preliminary Biological Assays. *Org. Lett. 8*, 6067-6070.

(13) Castillo, J. A., Guérard-Hélaine, C., Gutiérrez, M., Garrabou, X., Sancelme, M., Schürmann, M., Inoue, T., Hélaine, V., Charmatray, F., Gefflaut, T., Hecquet, L., Joglar, J., Clapés, P., Sprenger, G. A., and Lemaire, M. (2010) A Mutant D-Fructose-6-Phosphate Aldolase (Ala129Ser) with Improved Affinity Towards Dihydroxyacetone for the Synthesis of Polyhydroxylated Compounds. *Adv. Synth. Catal. 352*, 1039-1046.

(14) Szekrenyi, A., Soler, A. Garrabou, X., Guérard-Hélaine, C., Parella, T., Joglar, J., Lemaire, M., Bujons, J., and Clapés, P. (2014) Engineering the Donor Selectivity of D-Fructose-6-Phosphate Aldolase for Biocatalytic Asymmetric Cross-Aldol Additions of Glycolaldehyde. *Chem. Eur. J. 20*, 12572-12583.

(15) Güclü, D., Szekrenyi, A., Garrabou, X., Kickstein, M., Junker, S., Clapés, P., and Fessner, W.-D. (2016) Minimalist Protein Engineering of an Aldolase Provokes Unprecedented Substrate Promiscuity. *ACS Catal. 6*, 1848-1852.

(16) Yang, X., Ye, L., Li, A., Yang, C., Yu, H., Gu, J., Guo, F., Jiang, L., Wang, F., and Yu, H. (2017) Engineering of D-Fructose-6-Phosphate Aldolase A For Improved Activity Towards Cinnamaldehyde. *Catal. Sci. Technol. 7*, 382-386.

(17) Soler, A., Gutiérrez, M. L., Bujons, J., Parella, T., Minguillon, C., Joglar, J., and Clapés, P. (2015) Structure-Guided Engineering of D-Fructose-6-Phosphate Aldolase for Improved Acceptor Tolerance in Biocatalytic Aldol Additions. *Adv. Synth. Catal. 357*, 1787-1807.

(18) Rale, M., Schneider, S., Sprenger, G. A., Samland, A. K., and Fessner, W.-D. (2011) Broadening Deoxysugar Glycodiversity: Natural and Engineered Transaldolases Unlock a Complementary Substrate Space. *Chem. Eur. J. 17*, 2623-2632.

(19) Roldán, R., Sanchez-Moreno, I., Scheidt, T., Hélaine, V., Lemaire, M., Parella, T., Clapés, P., Fessner, W.-D., and Guérard-Hélaine, C. (2017) Breaking the Dogma of Aldolase Specificity: Simple Aliphatic Ketones and Aldehydes are Nucleophiles for Fructose-6-phosphate Aldolase. *Chem. Eur. J. 23*, 5005-5009.

(20) Junker, S., Roldan, R., Joosten, H.-J., Clapés, P., and Fessner, W.-D. (2018) Complete Switch of Reaction Specificity of an Aldolase by Directed Evolution *In Vitro*: Synthesis of Generic Aliphatic Aldol Products. *Angew. Chem. Int. Ed. 57*, 10153-10157.

(21) Guerard-Helaine, C., Debacker, M., Clapes, P., Szekrenyi, A., Helaine, V., and Lemaire, M. (2014) Efficient biocatalytic processes for highly valuable terminally phosphorylated C5 to C9 D-ketoses. *Green Chem. 16*, 1109-1113.

(22) Concia, A. L., Lozano, C., Castillo, J. A., Parella, T., Joglar, J., and Clapés, P. (2009) D-Fructose-6-phosphate Aldolase in Organic Synthesis: Cascade Chemical-Enzymatic Preparation of Sugar-Related Polyhydroxylated Compounds. *Chem. Eur. J. 15*, 3808-3816.

(23) The PyMOL Molecular Graphics System, Version 2.1 Schrödinger, LLC.

(24) Reetz, M. T., Wang, L.-W., and Bocola, M. (2006) Directed Evolution of Enantioselective Enzymes: Iterative Cycles of CASTing for Probing Protein-Sequence Space. *Angew. Chem. Int. Ed. 45*, 1236-1241.

(25) Miyoshi, N., Takeuchi, S., and Ohgo, Y. (1993) The SmI_2 Mediated Cross-Coupling Reaction of Aldehydes With α-Diketones in Their Aqueous Forms. *Chem. Lett. 22*, 2129-2132.

(26) Al-Smadi, D., Enugala, T. R., Norberg, T., Kihlberg, J., and Widersten, M. (2018) Synthesis of Substrates for Aldolase-Catalysed Reactions: A Comparison of Methods for the Synthesis of Substituted Phenylacetaldehydes. *Synlett 29*, 1187-1190.

(27) Tang, L. X., Gao, H., Zhu, X. C., Wang, X., Zhou, M., and Jiang, R. X. (2012) Construction of "Small-Intelligent" Focused Mutagenesis Libraries Using Well-Designed Combinatorial Degenerate Primers. *BioTechniques 52*, 149-158.

(28) Elfström, L. T., and Widersten, M. (2005) The *Saccharomyces cerevisiae* ORF YNR064c Protein Has Characteristics of an Orphaned Epoxide Hydrolase. *Biochim. Biophys. Acta 1748*, 231-221.

(29) Ma, H., Enugala, T. R., and Widersten, M. (2015) A Microplate Format Assay for Real-Time Screening for New Aldolases That Accept Aryl-Substituted Acceptor Substrates. *ChemBioChem 16*, 2595-2598.

(30) Blikstad, C., Dahlström, K. M., Salminen, T. A., and Widersten, M. (2013) Stereoselective Oxidation of Aryl-Substituted Vicinal Diols into Chiral α-Hydroxy Aldehydes by Re-Engineered Propanediol Oxidoreductase. *ACS Catal. 3*, 3016-3025.

(31) Gill, S. C., and von Hippel, P. H. (1989) Calculation of Protein Extinction Coefficients from Amino Acid Sequence Data. *Anal. Biochem. 182*, 319-326.

(32) www.simfit.org.uk

(33) Szrekenyi, A., Garrabou, X., Parella, T., Joglar, J., Bujons, J., and Clapés, P. (2015) Asymmetric Assembly of Aldose Carbohydrates From Formaldehyde and Glycolaldehyde By Tandem Biocatalytic Aldol Reactions. *Nat. Chem. 7*, 724-728.

(34) Tittman, K. (2014) Sweet Siblings With Different Faces: the Mechanisms of FBP and F6P Aldolase, Transaldolase, Transketolase and Phosphoketolase Revisited in Light of Recent Structural Data. *Bioorg. Chem. 57*, 263-280.

(35) Schneider, S., Sandalova, T., Schneider, G., Sprenger, G. A., and Samland, A. K. (2008) Replacement of a Phenylalanine by a Tyrosine in the Active Site Confers Fructose-6-Phosphate Aldolase Activity to the Transaldolase of *Escherichia coli* and Human Origin. *J. Biol. Chem. 283*, 30064-30072.

(36) Rose, I. A., O'Connell, E. L., and Mehler, A. H. (1965) Mechanism of the Aldolase Reaction. *J. Biol. Chem. 240*, 1758-1765.

(37) Bender, M. L., and Williams, A. (1966) Ketimine Intermediates in Amine-Catalyzed Enolization of Acetone. *J. Am. Chem. Soc. 88*, 2502-2508.

(38) Fersht, A. (1999), in Structure and Mechanism in Protein Science, pp 114−116, W. H. Freeman, New York.

(39) Bar-Even, A., Milo, A., R., Noor, E., and Tawfik, D. S. (2015) The Moderately Efficient Enzyme: Futile Encounters and Enzyme Floppiness. *Biochemistry 54*, 4969−4977.

(40) Baś, S., Woźniak, Ł., Cygan, J., and Mlynarski, J. (2013) Asymmetric *syn*-Aldol Reaction of α-Hydroxy Ketones with Tertiary Amine Catalysts. *Eur. J. Org. Chem.*, 6917-6923.

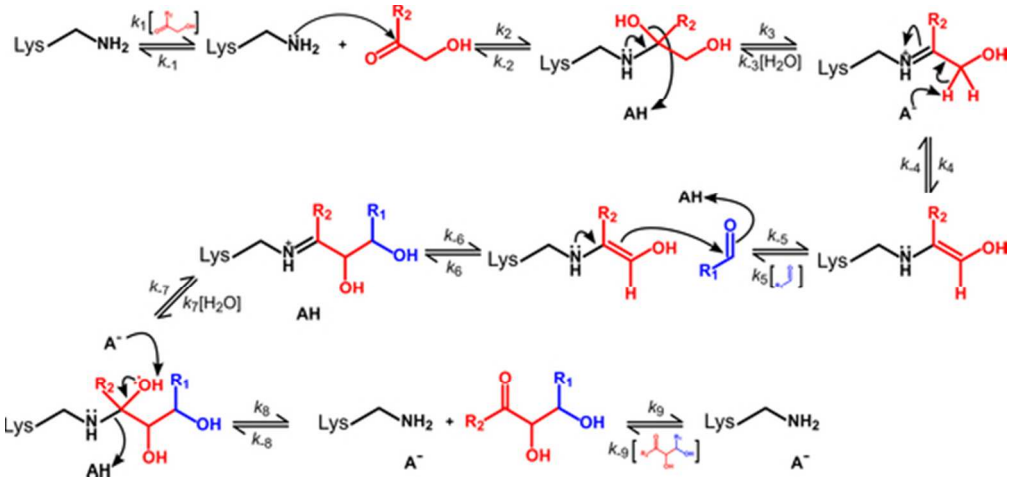

49x23mm (300 x 300 DPI)

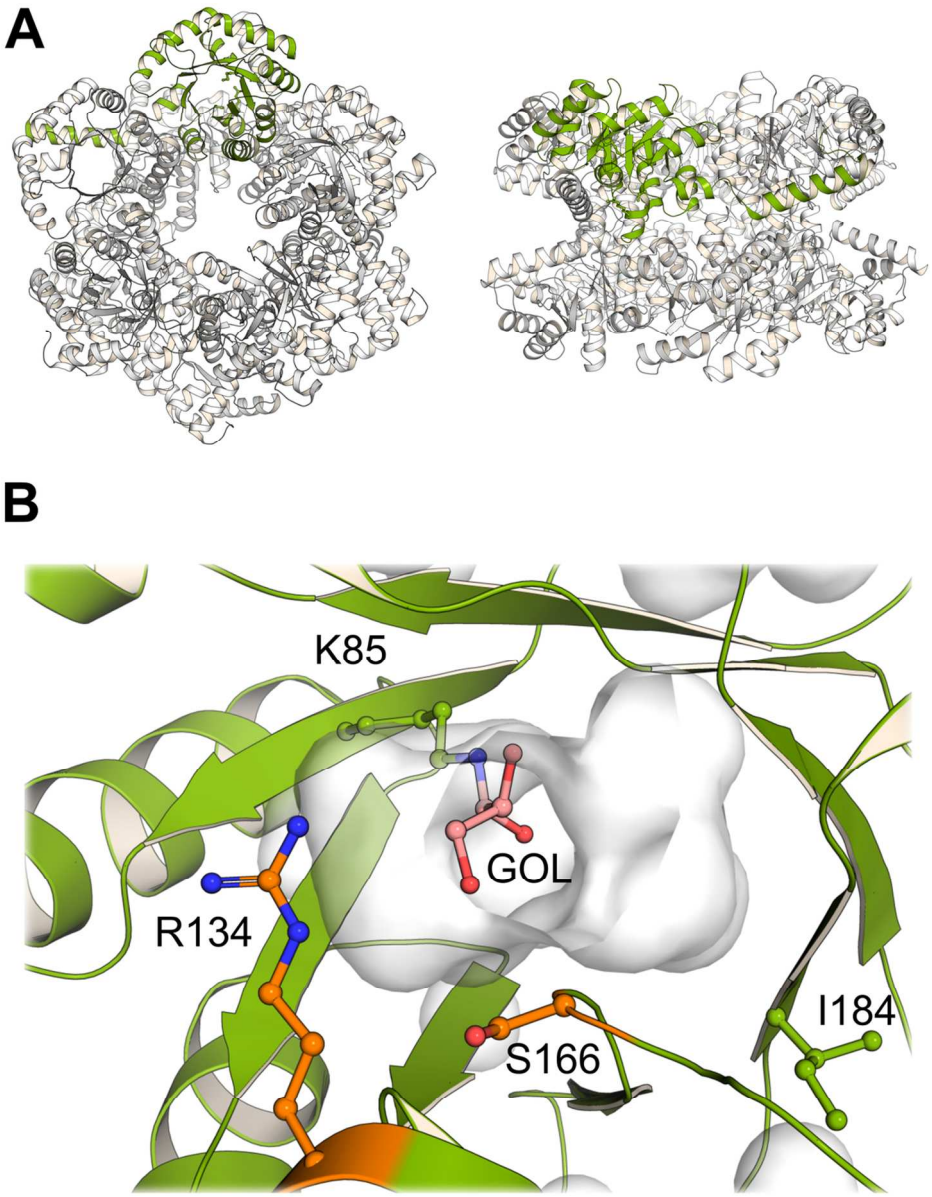

108x138mm (300 x 300 DPI)

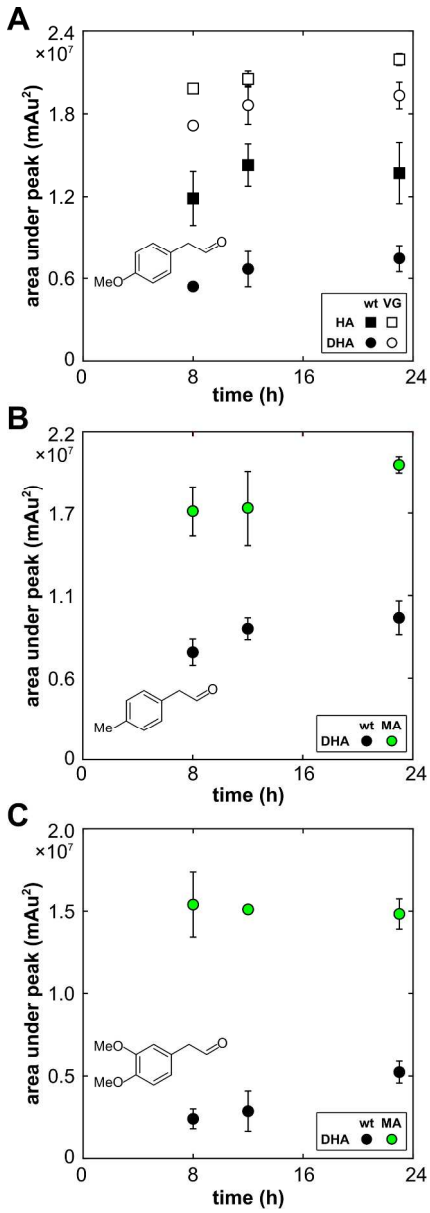

182x521mm (300 x 300 DPI)

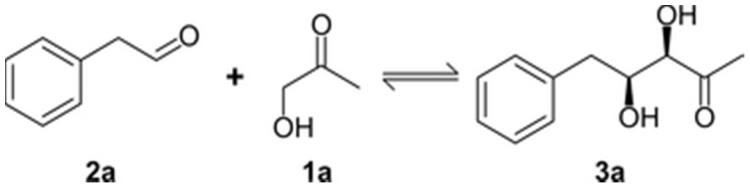

31x7mm (300 x 300 DPI)

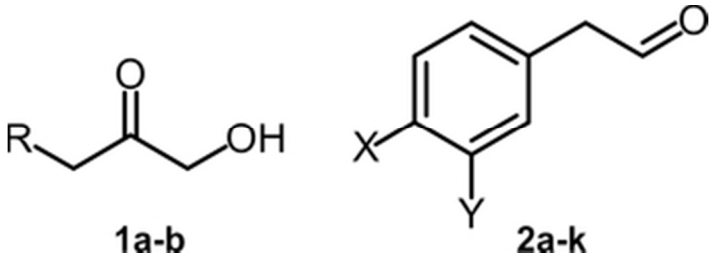

29x10mm (300 x 300 DPI)

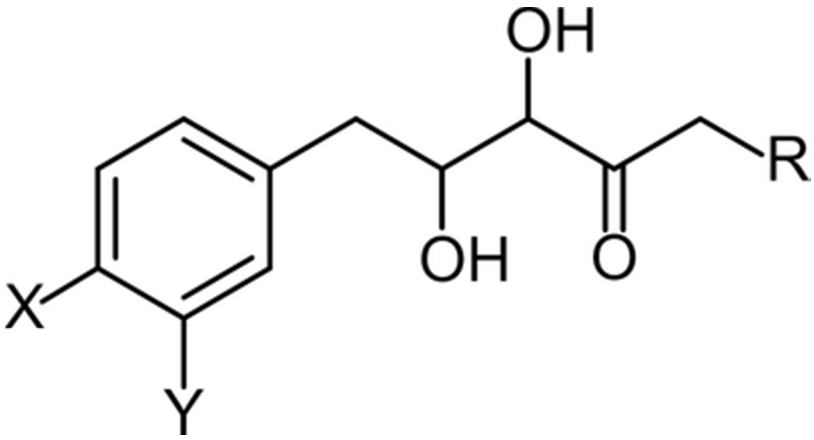

34x18mm (300 x 300 DPI)

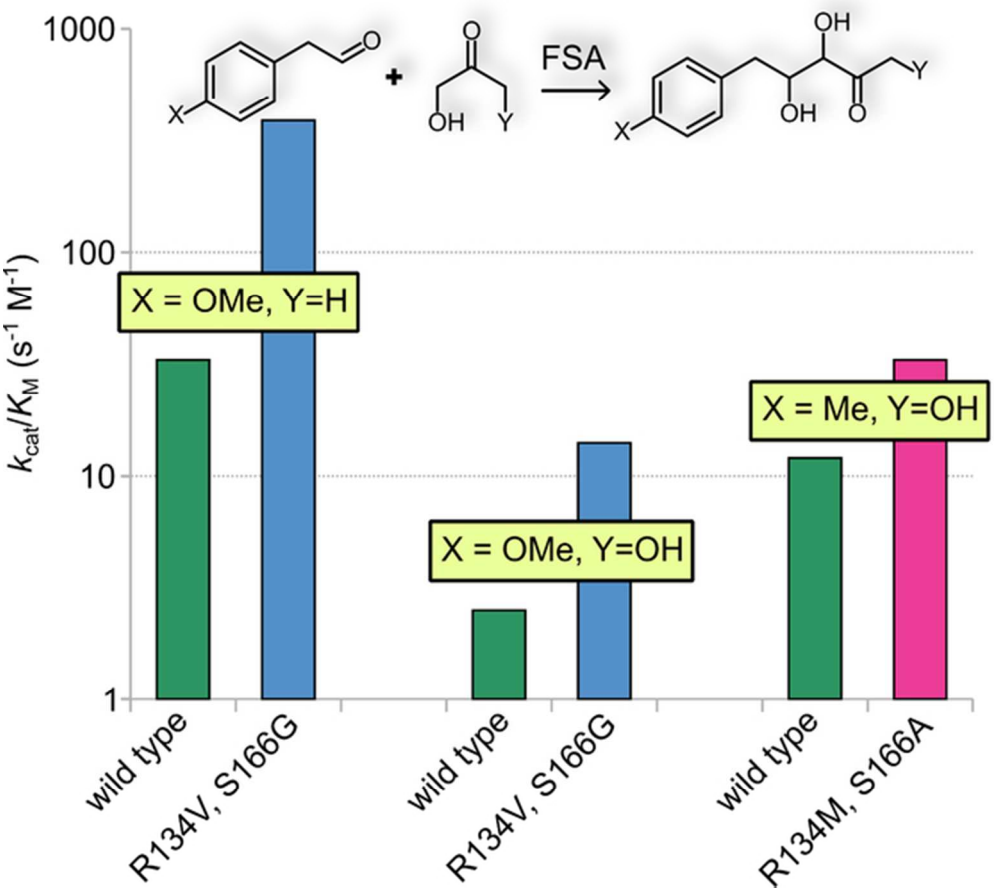

56x49mm (300 x 300 DPI)